

LOCAL AND GENERAL MONITORING OF FORNI GLACIER (ITALIAN ALPS) USING MULTI-PLATFORM STRUCTURE-FROM-MOTION PHOTOGRAMMETRY

M. Scaioni ^{a,*}, M. Corti ^a, G. Diolaiuti ^b, D. Fugazza ^b, M. Cernuschi ^c

^a Dept. of Architecture, Built environment and Construction engineering (ABC), Politecnico Milano
via Ponzio 31, 20133 Milano, Italy – marco.scaioni@polimi.it

^b Department of Environmental Science and Policy (DESP), Università degli studi di Milano
via Mangiagalli 34, 20133 Milano, Italy – {guglielmina.diolaiuti, davide.fugazza}@unimi.it

⁴Agricola 2000 S.C.P.A., 20067 Tribiano (MI), Italy – massimo.cernuschi@gmail.com

KEY WORDS: Forni Glacier, Glaciology, Photogrammetry, Quality Assessment, Structure-from-Motion, UAV/UAS

ABSTRACT:

Experts from the University of Milan have been investigating Forni Glacier in the Italian alps for decades, resulting in the archive of a cumbersome mass of observed data. While the analysis of archive maps, medium resolution satellite images and DEM's may provide an overview of the long-term processes, the application of close-range sensing techniques offers the unprecedented opportunity to operate a 4D reconstruction of the glacier geometry at both global and local levels. In the latest years the availability of high-resolution DEM's from stereo-photogrammetry (2007) and UAV-photogrammetry (2014 and 2016) has allowed an improved analysis of the glacier ice-mass balance within time. During summer 2016 a methodology to record the local disruption processes has been investigated. The presence of vertical and sub-vertical surfaces has motivated the use of Structure-from-Motion Photogrammetry from ground-based stations, which yielded results comparable to the ones achieved using a long-range terrestrial laser scanner. This technique may be assumed as benchmarking for accuracy assessment, but is more difficult to be operated in high-mountain areas. Nevertheless, the measurement of GCP's for the terrestrial photogrammetric project has revealed to be a complex task, involving the need of a total station a GNSS. The effect of network geometry on the final output has also been investigated for SfM-Photogrammetry, considering the severe limitations implied in the Alpine environment.

1. INTRODUCTION

1.1 Application of photogrammetry in Geosciences

The innovation related to the great contribution that laser scanning and photogrammetric techniques have given to the Geosciences is today clearly evident. This success is motivated on one side by the need of detailed, accurate and complete 3D digital surface models, on the other by the technological development undergone in the last 15 years. Even though photogrammetry has already provided an important contribution in Geoscience applications during '90 (see, e.g., Lane et al., 1993), starting from the first decade of the new century the laser scanning techniques seemed to be the master solution to the problem of 3D modelling (see, e.g., Heritage and Large, 2009; Jaboyedoff et al., 2012). Surprisingly, the important outputs of Computer Vision recently opened a new era for photogrammetry, thanks to the development of fully automatic methods for image orientation (Barazzetti et al., 2011) and dense surface reconstruction (Eltner et al., 2016). These new solutions have established what is commonly referred to with the term 'Structure-from-Motion' (SfM) Photogrammetry (Westoby et al., 2012). Using a consumer-grade camera equipped with an adequate focal lens, and using a suitable block structure, it is possible to obtain a 3D model of topographic surfaces on the basis of a purely image-based approach. A total station or GNSS sensors are needed for the measurement of a few points for geo-referencing the resulting point cloud into a give reference frame. When the absolute geo-referencing is not required (e.g., when studying some local

morphologies as in Käab et al., 2014) the presence into the scene of natural or artificial baselines with known length may suffice for scaling the whole point cloud.

The light weight of camera sensors allows their transportability on Unmanned Aerial Systems (UAS) as well (Colomina & Molina, 2014; Carbonneau & Dietrich, 2016; O'Connor et al., 2017). This opens the possibility to survey large areas with a nadir view or to reach areas that may not be accessible from the ground. In fact, while satellite remote sensing is expected to provide the major contribution for monitoring and investigation long time-scale changes at medium/low spatial resolution (Scaioni et al., 2014), in many projects a higher level of detail is necessary. Whilst the use of sensors on manned aircrafts may fulfill these requirements, the costs involved and possible operational criticalities (e.g., due to safety concerns, flight regulations, distance from the aircraft base) may prevent their application. On the other hand, UAS represent an interesting compromise between the required accuracy/resolution and budgetary problems. In some cases the acquisition of a ground-based photogrammetric network may be also required, for example for 3D reconstruction of vertical and sub-vertical surfaces. For the sake of completeness, the capability of some UAS to acquire oblique images may open unprecedented opportunities to model vertical regions as well. Given a suitable geodetic reference, multi-platforms surveys may be integrated to obtain full 3D models which completely depict geomorphic objects under different point of views.

1.2 SfM and UAS's for glaciological studies

In the field of glaciological studies the potential of SfM-photogrammetry from ground-based networks and UAS's has been already exploited in a few case studies, but an even more impressive widespread of its applications is expected during next years. Some examples related to the use of UAS solutions are reported in Solbø & Storvold (2013), Whitehead et al. (2013), Immerzeel et al. (2014), Tonkin et al. (2014), Bülher et al. (2015), Fugazza et al. (2015), Ryan et al., (2015), Clapuyt et al. (2016), Dall'Asta et al. (2016), Kraaijenbrink et al. (2016). In addition, Bhardwaj et al. (2016) give an overview about the application of UAS in Glaciology. In Gómez-Gutiérrez et al. (2014; 2015) and Piermattei et al. (2015; 2016) the application of ground-based photogrammetric networks within SfM techniques are investigated to reconstruct Alpine glaciers.

As generally happens in Geosciences, in Glaciological studies satellite remote sensing may provide data sets for medium/long-term regional investigations of geometric (see, e.g., Heid & Käab, 2012) as well as radiometric aspects (see, e.g., Fugazza et al., 2016), which are the solely way to study those areas difficult to be accessed such as Arctic and Antarctic regions (see, e.g., Scaioni et al., 2013; Gu et al., 2014). The availability of long archives recorded during the past decades also allows for retrospective analyses (see, e.g., Li et al., 2017). But in many cases, the necessity of detailed models requires local surveys based on terrestrial or UAS acquisition. The specific environmental and geomorphic characteristics of glacier regions represent a challenge for the use of any in-situ surveying techniques, including UAS that, however, need to be taken off, operated and landed in the nearby of the region under investigation. This results in the fact that in many cases the ideal operational conditions, the perfect image-block geometry and properties may not be pursued as in typical applications of close-range photogrammetry in controlled environment, see Luhmann et al. (2014).

In this paper the aim is not to revise the SfM application in the field of Glaciology, since the main issues have been already addressed in other recent papers. Eltner et al. (2016) provide a quite complete and up-to-date review about this topic. Here the focus is to highlight some issues related to the application of SfM photogrammetry to the study of changes in alpine glaciers. In particular some experiences carried out on Forni Glacier (Italian Alps) are reported and discussed (see Sect. 2).

2. THE STUDY OF FORNI GLACIER IN THE ITALIAN ALPS

2.1 Presentation of the case study

Forni Glacier (Ortles Cevedale mountain group) in the National Stelvio Park (Northern Italy) is one of the major storage of ice in the Italian Alps, which is currently suffering from a quick ablation process under the global climate change condition. The latest Italian Glacier Inventory (Smiraglia et al., 2015) reported the total glacier area as 11.34 km², an altitudinal range between 2501 and 3673 m a.s.l., and a North-North-Westerly aspect. Since this inventory was based on 2007 data, the successive separation of the multiple ice tongues, the loss of ice bulk at global level and the retreat resulted in a reduction of the

reported extension (Azzoni et al., 2017). These are progressive processes that have been active in the latest decades but recently they have been showing a quick acceleration (D'Agata et al., 2014). Just to give an idea of the magnitude of the retreat process, during the Little Ice Age (LIA), which approximately extended from 1500-1850 B.C., Forni Glacier spanned over an area of 17.80 km² (Diolaiuti & Smiraglia, 2010). On the other sides, some sectors of the lower part of glacier's main tongue are undergoing a local disruption process entailing first the formation of circular crevasses, to be followed by their collapse and the formation of large exposures of bedrock. An example can be seen in the central part of Figure 3. Such local processes are quite fast to develop: from their preliminary events to the full ice collapse the process may take less than one year to be accomplished. Monitoring the ice degradation process from a quantitative and qualitative point-of-view is of great importance for understanding the related dynamics and to apply rigorous numerical models. While the analysis of archive maps, medium resolution satellite images and DEM's may provide an overview of the long-term processes, the application of close-range sensing techniques (see Rutzinger et al., 2016) from ground-based and UAV stations offers the unprecedented opportunity to operate a 4D reconstruction of the glacier geometry at both global and local levels. Recent research on this glacier can be found in Fugazza et al. (2015; 2016; 2017) and Azzoni et al. (2016).



Fig. 1 - Forni Glacier and its geographic position in the Italian Alps.

2.2 Data sets

Six photogrammetric data sets have been used in this study, to be integrated and continued in the future for monitoring purpose.

2.2.1 Aerial photogrammetry (2007). A digital elevation model (DEM) was obtained from an aerial photogrammetric mission operated with a digital push-broom camera Leica ADS40. Dating back to 2007, this data set is the oldest high-resolution digital data source covering the full glacier and periglacial area. The flight was operated during the 2007 TerraItaly project by the BLOM C.G.R company. A flight height of 6,300 m was followed with an average GSD (ground sample distance) of 65 cm over the entire Lombardia Region. After photogrammetric stereo-processing, a DEM was generated with a cell resolution of 2 m x 2 and a vertical accuracy (reported by the company) of ± 3 m.

2.2.2 UAS missions (2014 and 2016). Two UAS flights covering the glacier terminus were operated in 2014 and 2016 (Fugazza et al., 2017), respectively.

The 2014 UAV survey covered both the terminus of the central and eastern ablation tongue of Forni Glacier. This flight was operated on 28th August 2014 using a SenseFly SwingletCam fixed wing aircraft. A Canon Ixus 127 HS compact camera (16 Mpix sensor size, 4.3 mm focal length) was implemented in the payload. The UAS was flown at a relative flying height of approx. 380 m above the average glacier surface, which resulted in an average GSD of 12 cm. A quite regular along-strip overlap of 70% was obtained, while sidelap was not regular because of the varying surface topography, but ranged around 60%. The flight was operated in the early morning (07:44-8:22 AM) in order to work in diffuse lighting conditions and reduced wind speed. In addition, the presence of tourists on the glacier is reduced during this time of the day. No GCP's were available during this flight. The only information for absolute geo-referencing were the camera-pose locations obtained from the onboard navigation-grade GNSS sensor. The uncertainty of GNSS direct positioning resulted in a global bias for the geo-products obtained from this block in the order of ± 2 m. More pieces of information may be retrieved in Fugazza et al. (2015).

The 2016 UAV was operated across two days (30th August and 1st September 2016), because the weather conditions limited the operational time windows. Being not possible to fly in the early morning, the central hours of both days were selected. The presence of low cloud cover avoided the direct solar radiation on the glacier surface while preserving diffuse illumination conditions. The UAS employed in this survey was a customized quadcopter incorporating a Tarot frame 650 size, VR Brain 5.2 Autopilot & APM Arducopter 3.2.1 Firmware. A Canon Powershot ELPH 320 HS compact camera (16 Mpix sensor size, 4.3 mm focal length) was implemented in the payload. A low relative altitude of 50 m with respect to the topographic surface was selected, which ensured an average GSD=5.7 cm. Several individual parallel flights were conducted to cover a small section of the proglacial plain and different surface types on the glacier surface, including the terminus, a collapsed area on the central tongue, the eastern medial moraine and some debris-covered parts of the eastern tongue. An overlap of approximately 70% was obtained along both along- and across-strip directions. Eight GCP's were deployed on the glacier terminus and in the periglacial area in front of it (see Fig. 2). Such GCP's, made up of white and red targets (size 80 cm x 80 cm) recognizable in the images, were measured by using a RTK-GNSS sensor. Since of the higher power consumption of quadcopter, the surveyed area had a smaller size (see also Bhardwaj et al., 2016). In addition, multiple missions were necessary to accomplish the whole project, each of them requiring a taking off/landing site close to the portion of the flight plan to be operated. The camera-poses and the reconstructed for the 2016 UAS flight are reported in Figure 2, while more details about this mission are reported in Fugazza et al. (2017).

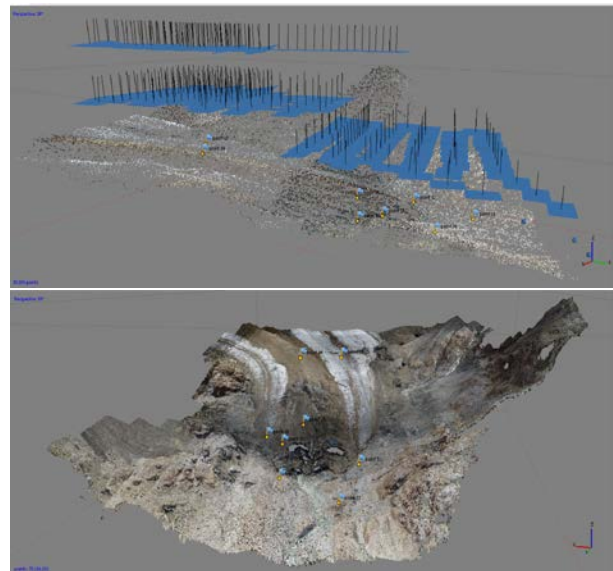


Fig. 2 - On the top: structure of the photogrammetric block captured during 2016 UAS mission; at the bottom: point cloud obtained after photogrammetric processing and positions of GCP's.

2.2.3 Terrestrial Photogrammetry. The latest three data sets consisted in multiple blocks obtained from ground-based photogrammetric networks. The acquisition time was concurrent with the 2016 UAS flight. An SLR (single lens reflex) camera Nikon D700 was used for image acquisition, equipped with a full-frame CMOS sensor (4256x2823 pix) and a 50-mm lens.

Four independent blocks of images were captured with the purpose of reconstructing different parts of Forni Glacier:

1. Block 1: the glacier terminus including the rock flanks, a part of the periglacial area, and the ending part of the central moraine over the main glacier tongue (Fig. 3a);
2. Block 2: an area of the glacier in correspondence of a rock outcrop formed as consequence of ice thickening (Fig. 3b); and
3. Block 3: the hung terminus of one of the eastern ice tongues that separated from the main glacier body (see Fig. 3c).

A preliminary planning of the image networks for each of these photogrammetric blocks was not possible, because the local topography, the distances involved and the presence of unstable or dangerous areas did not allow to collect images in ideal positions. Thus, the criterion applied for establishing the camera stations was to explore as many positions as possible from which the targeted region could be observed from different viewpoints. In particular, to optimize the SfM process, an attempt to find a trade-off between long baselines with convergent images (providing a better intersection of corresponding rays) and short-baseline with parallel images



Fig. 3. Three parts of Forni Glacier that were separately targeted in ground-based photogrammetric networks.

(helping the dense matching stage) was made according to Wenzel et al. (2013). In the case of Block 1 which had the target to reconstruct a very large and irregular surface, images had also largely variable scales.

Seven natural features were selected as GCP's on the glacier front for geo-referencing of Block 1. Their coordinates in the geodetic reference frame were measured using a theodolite equipped with a reflector-less rangefinder. This operation turned out to be quite tedious and complex. In addition, the recognition of these GCP's on the images was also a critical task, that probably resulted in degrading the accuracy of geo-referencing. The position and heading of the theodolite station in the geodetic reference frame was found by linking a couple of RTK-GNSS GCP's. Blocks 2 and 3 were only roughly scaled using some baselines with known length.

In addition, some laser scans were captured by means of a long-range terrestrial laser scanner Riegl LMS-Z420i. Notwithstanding the operating range (theoretically up to 800 m in highly reflective conditions), the long distances involved prevented the acquisition of laser point clouds corresponding to Blocks 2 and 3. In the case of Block 1, a point cloud was scanned to reconstruct the front of the glacier terminus, and to be used for validation of photogrammetric point clouds (see Fugazza et al., 2017).

2.3 Photogrammetric processing

All photogrammetric blocks were processed using the same pipeline. In a first stage, SfM was applied to extract tie points (TP's) and compute the approximate exterior orientation (EO) of the images, to be fed into a bundle adjustment including camera self-calibration and GCP observations or baselines for scaling. Secondly, a pixelwise dense matching technique was adopted for deriving the point cloud describing the surface of the region of interest. This workflow was operated using the popular Agisoft Photoscan version 1.2.4 (www.agisoft.com). Since no GCP's were measured during the 2014 UAS campaign, the registration of this data set into the geodetic frame was based on GNSS navigation data only. In the case of both UAS blocks, navigational observations were used as approximate values for the SfM pipeline. This option allows to shorten the number of potential overlapping images and to reduce the computational burden. Agisoft Photoscan allows to setup a level of accuracy for both SfM and dense matching phases, which corresponds to the use of the images at native or

sub-sampled resolution. The EO has been always computed at the highest accuracy level ('Very-high'), while the dense matching was computed at the second-best option ('High'). Indeed, from the experience of the authors, the highest level involves a much longer computation time, which does not correspond to a proportional improvement of the accuracy. Figure 4 displays some views of point clouds obtained from Blocks 1, 2 and 3.

After the generation of the point cloud, a grid DEM and orthoimage were produced from each of both UAS blocks. Block 1 from ground-based photogrammetry was merged with the point cloud from 2016 UAS flight. The resulting point cloud was then subsampled at 20 cm spatial resolution to obtain a complete 3D model of the Forni Glacier terminus. The main characteristics of this model is the high resolution on one side, which allows the interpretation of surface features (crevasses, roughness, dip orientation). On the other, the integration of a point cloud obtained from airborne vertical images to another one from ground-based camera stations, allows to improve the reconstruction of surfaces with different spatial orientation such as those typical of the glacier terminus.

2.4 Accuracy evaluation

In general, to evaluate the quality of a photogrammetric process, two different types of analyses are possible. The first one concerns the scrutiny of photogrammetric metrics, mainly related to the output of Least-Squares bundle adjustment (RMSE of image coordinate residuals, GCP 3D residuals in object space, multiplicity of corresponding rays, estimated theoretical accuracy of TP's and EO parameters). As it is well known from the theoretical background of analytical photogrammetry, these figures are significant only in the case the photogrammetric network is based on manifold TP's, i.e., the same points have been recognized and matched on more than two images. In theory, the obtained theoretical accuracy should be at the same order of the expected ones. Unfortunately, the complexity of photogrammetric networks operated in the case of glacier surveys makes difficult to forecast the theoretical accuracy, as for instance in the normal case of stereo-photogrammetry, see Luhmann et al. (2014).

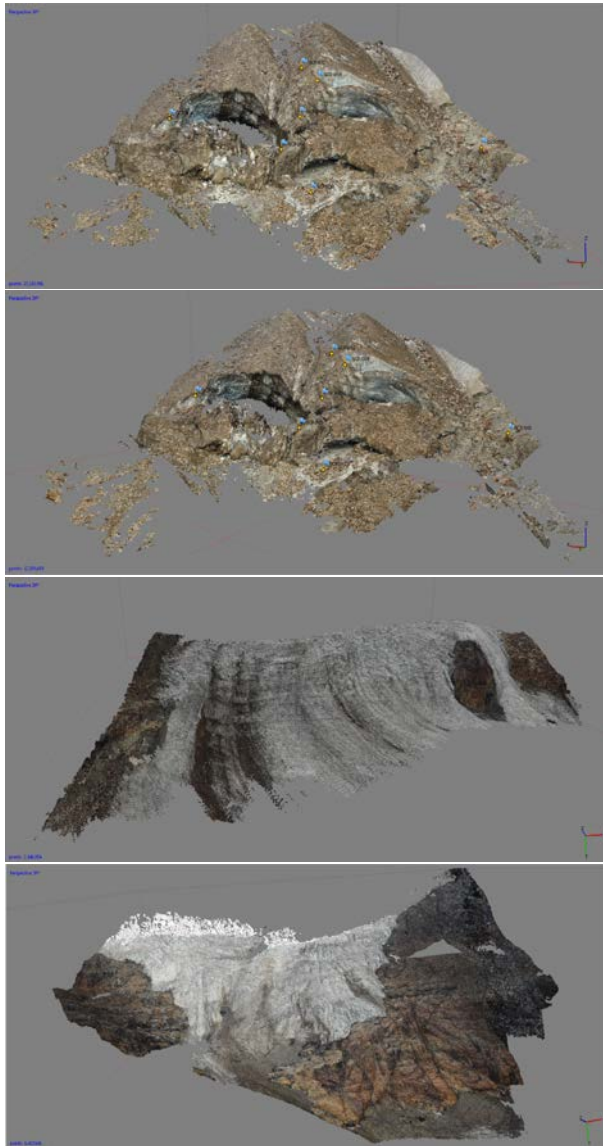


Fig. 4. Point clouds obtained after dense matching colored using RGB information from images; from top to bottom: Block 1 ('complete image set'), Block 1 ('reduced image set'), Block 2, Block 3.

Even though alternative formulas have been proposed to deal with multi-view photogrammetric blocks including convergent poses (see the discussion in Eltner et al., 2016), their practical use is quite complex because of the two many variables to be guessed case-by-case. On the other side, the availability of a few independent check points (ChkP) is a solid method for assessing the metric quality of a photogrammetric block. Unfortunately, the measurement of geodetic points to be used as GCP's or ChkP's may typically be a quite complex task in the mountain environment. In project like the one under discussion here, the preference was given to the use of all geodetic points as GCP's, due to the limited number.

In the case of point cloud accuracy, the first approach is not viable since in general no theoretical accuracy figures are provide after dense matching. An innovative solution to cope with this problem through the production of 'precision maps' for the obtained point clouds has been recently published in James et al. (2017). This method opens the door for SfM practitioners to carry out the comprehensive quality analysis typical of analytical photogrammetry. On the other hand, this method has not been applied yet to the blocks analyzed here. The unique solution is represented by comparing the output point clouds with benchmarking data sets, such as high-precision geodetic points or surfaces (Eltner et al., 2016). Where available, the TLS point clouds have been used as benchmark for assessing the accuracy of photogrammetric point clouds.

The RMSE (Root Mean Square Error) of residuals on GCP's (34.4 cm) demonstrated that a bias existed between computed point clouds and the geodetic reference frame. This result does not have any significant influence on the analysis based on this data set for long term monitoring of the glacier retreat, since its dynamic is quite fast. These results are also similar to the ones of analogue projects, such as the ones reported in Piermattei et al. (2015; 2016) for the ground-based photogrammetric surveys of two small Italian glaciers. On the other hand, due to the complexity of measurement operations both in the field and on the images, some doubts about the absolute accuracy of GCP's are reasonable. Alternative options are, in the case of terrestrial photogrammetry, the direct measurement of the position of a few camera stations to be used as ground constrain (see Forlani et al., 2014; 2015). A similar system is under development to be use for future measurement campaigns on the Forni Glacier. In the case of UAS flights, the employ of a GNSS-RTK sensor on-board may directly provide a sufficient quality exterior orientation. Dall'Asta et al. (2016) report about RMSE in the order of 4 cm and 7 cm that have been evaluated for position and elevation, respectively.

2.5 Influence of photogrammetric network geometry

Two opposite structures for the photogrammetric network are suggested in the literature: (i) Piermattei et al. (2015) report that a large number of photos with short baselines are preferably to fewer photos with longer baselines; (ii) Mosbrucker et al. (2017) suggest prioritizing the image quality over the image number, by acquiring the minimum number of photos to cover the study area and to avoid occlusions. In order to answer this question, all terrestrial photogrammetric blocks (1, 2, 3) were acquired by using strategy (i), but a second version ('reduced image set') was then selected to be representative of configuration (ii). In the selection process, the function 'Estimate image quality' implemented in Agisoft Photoscan was used to scrutinize those images with focusing problems, lack of texture and the like. This resulted in approximately halving the number of images in the output 'reduced image sets.' The structure of camera poses for both configurations in the case of Block 1 are depicted in Figure 5.

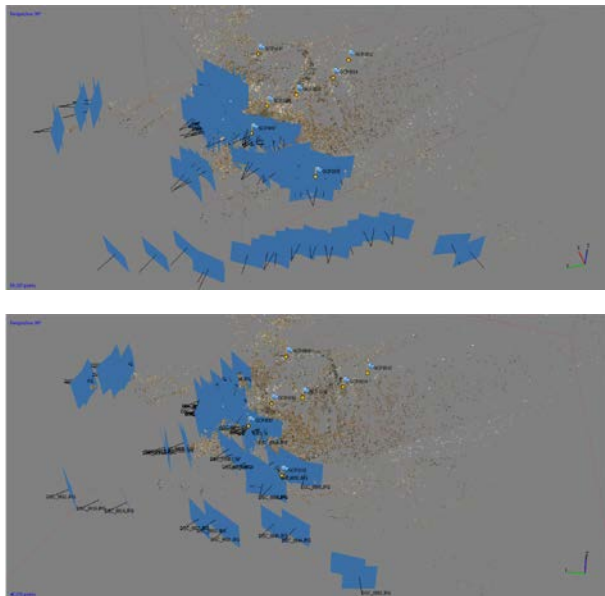


Fig. 5. Camera pose network for Block 1: in the upper image with ‘complete image set,’ in the lower image with ‘reduced image set.’

In Table 1, some parameters have been reported to analyze the differences between the blocks in both configurations. First of all, the total number of extracted TP’s is not reduced in a way proportional to the reduction of the images. Indeed, the drop in the TP number ranges from 22% to 44%. This result is theoretically sound since TP’s in object space depend on the extension and texture of the surveyed area as well as on the camera pose geometry, but not on the number of images. The average number of projections (rays) per point has an uneven behavior in all the blocks, also with a case (Block 2) where it has increased. Anyway, in Blocks 1 and 2 a safe value has been obtained (4.5-4.3), while in Block 3 is quite low (2.6). This parameter is quite important since it directly controls the local redundancies of the observations and then the inner reliability of the observations (Luhmann et al., 2014). Considering the average number of TP’s per image, in general the ‘reduced image sets’ show a higher value. Anyway, the number of TP’s is always more than sufficient, also in the images with the minimum number (727 TP’s in one image of Block 3). The RMSE of TP residuals on the images after reprojection is always quite small, either in ‘complete’ (0.2-0.3 pix) and in ‘reduced image sets’ (0.1-0.2 pix). The effective image overlap, which gives the number of overlapping images in the reconstructed surface, has a drop as expected, but it ranges from 13% to 39%. This range is much lower than the fraction of excluded images in the ‘reduced’ blocks. In the case of Block 1 which entails the use of GCP’s, only a slightly change in the RMSE on 3D residuals can be noticed. The number of points in the final point clouds dropped down between 37% and 55%. This has been the most significant change, supporting for the use of strategy (i).

According to this outcome, the network geometry, the image quality and the ground control represent the most important factors controlling the quality of the main

photogrammetric output. Less important influencing factors have resulted to be the surface texture and the type of substrata (snow, firn and debris), as also reported by Piermattei et al. (2015).

Block 1				
		‘complete’	‘reduced’	change (%)
#images		134	70	-48
#tie points (TP’s)		59k	46k	-22
Avg. rays per TP		5.6	4.5	-20
#TP’s per image	Avg.	2455	2946	+20
	Min.	744	1031	+39
RMSE of TP reprojection [pix]	Avg.	0.3	0.2	-33
	Max.	0.7	0.4	-43
Effective image overlap		7.2	5.3	-26
3D RMSE on GCP’s [cm]		34.4	32.5	-5
#points of point cloud		27.1M	12.3M	-55

Block 2				
		‘complete’	‘reduced’	change (%)
#images		29	15	-48
#tie points (TP’s)		16k	9k	-44
Avg. rays per TP		3.9	4.3	+10
#TP’s per image	Avg.	2131	2653	+24
	Min.	572	1787	+212
RMSE of TP reprojection [pix]	Avg.	0.2	0.2	0
	Max.	0.3	0.3	0
Effective image overlap		5.4	4.7	-13
#points of point cloud		2.1M	1.0M	-52

Block 3				
		‘complete’	‘reduced’	change (%)
#images		37	18	-51
#tie points (TP’s)		29k	20k	-31
Avg. rays per TP		3.4	2.6	-23
#TP’s per image	Avg.	2657	2909	+9
	Min.	1378	727	-47
RMSE of TP reprojection [pix]	Avg.	0.3	0.2	-33
	Max.	0.2	0.1	-50
Effective image overlap		4.0	2.8	-30
#points of point cloud		6.4M	4.0M	-37

Table 1. Properties and results of photogrammetric processing in the case of ‘complete image sets’ and ‘reduced image sets’ for ground-based image networks.

2.6 Analysis of glacier changes

The 2007 DEM (2 m x 2 m resolution) and two DEM’s generated from the photogrammetric point clouds obtained from 2014 and 2016 UAS flights (60 cm x 60 cm resolution) were compared to evaluate changes. When comparing 2007 DEM with others, these were resampled at the same spatial resolution. In addition, a procedure for co-registering DEM’s following Berthier et al. (2007) was applied. DEM differencing enhanced a generalized thinning of Forni Glacier tongue over the entire study period (2007-2016). After computing the differences in terms of volumes, the mean ice density (0.917 g/cm³) was used for evaluating the geodetic mass balance. Mean annual values of -4.17±0.22 my⁻¹ water equivalent (w.e.)

between 2007 and 2014 and $-4.36 \pm 0.27 \text{ m y}^{-1}$ w.e. between 2007 and 2016 over the lower part of the glacier tongue were found. This result suggests that thinning over 2014–2016 was higher than between 2007 and 2014. Here the mean thickness change of the glacier tongue was $-5.20 \pm 1.11 \text{ m y}^{-1}$ with a maximum surface elevation change of -38.71 m . More details including maps of changes, comparison with historical values and considerations about the spatial distribution of variations may be found in Fugazza et al. (2017). Here the readers may also find some statistical analysis on the quality of photogrammetric point clouds in selected windows, and the comparison with benchmarking data from terrestrial laser scanning. It is also shown how the integration of UAS and ground-based photogrammetric data may provide a complete description of the complex topographic surface of Forni Glacier.

5. CONCLUSIONS AND FUTURE WORK

In this study the potential of UAS and terrestrial 'Structure-from-Motion' photogrammetry has been evaluated for monitoring changes of Forni Glacier in the Italian Alps. By comparing different DEM's of the glacier tongue from UAS flights in 2014 and 2016, and considering a DEM from aerial photogrammetry derived from 2007 data, an increased rate of glacier ablation was found in recent years, reaching $-5.20 \pm 1.11 \text{ m a}^{-1}$ between 2014 and 2016. Ground-based photogrammetry was used to reconstruct some portion of the glacier from a terrestrial point-of-view, which plays an important role in modeling vertical regions.

Close-range surveys from UAS and ground-based platforms are supposed to be repeated in the future for both long-term (annual basis) and short-term (monthly basis, only during summer) to better depict global and local phenomena contributing to the acceleration of the glacier ablation process.

Acknowledgements

This study was funded by DARAS (Presidency of the Council of the Italian Government). The authors acknowledge the Central Scientific Committee of CAI (Italian Alpine Club) and Levissima San Pellegrino S.P.A. for funding the UAV quadcopter. The authors also thank Stelvio Park Authority for the logistic support and for permitting the UAV surveys and IIT Regione Lombardia for the provision of the 2007 DEM. Acknowledgements also go to the GICARUS lab of Politecnico Milano at Lecco Campus. Finally, the authors would also like to thank Tullio Feifer, Livio Piatta, and Andrea Grossoni for their help during field operations.

REFERENCES

References from journals:

Azzoni, R.S., Senese, A., Zerboni, A., Maugeri, M., Smiraglia, C., Diolaiuti, G.A., 2016. Estimating ice albedo from fine debris cover quantified by a semi-automatic method: the case study of Forni Glacier, Italian Alps. *Cryosphere*, 10: 665-679, doi:10.5194/tc-10-665-2016.

Azzoni, R.S., Fugazza, D., Zennaro, M., Zucali, M., D'Agata, C., Maragno, D., Cernuschi, M., Smiraglia, C., Diolaiuti, G.A., 2017. Recent structural evolution of Forni Glacier tongue (Ortles-Cevedale Group, Central Italian Alps). Submitted to *Journal of Maps*.

Berthier, E., Arnaud, Y., Kumar, R., Ahmad, S., Wagnon, P., Chevallier, P., 2007. Remote sensing estimates of glacier mass balances in the Himachal Pradesh (Western Himalaya, India). *Remote Sensing of Environment*, 108: 327-338.

Bhardwaj, A., Sam, L., Akanksha, Martin-Torres, F.J., Kumar, R., 2016. UAVs as remote sensing platform in glaciology: Present applications and future prospects, *Remote Sensing of Environment*, 175: 196-204.

Bühler, Y., Marty, M., Egli, L., Veitinger, J., Jonas, T., Thee, P., and Ginzler, C., 2015. Snow depth mapping in high-alpine catchments using digital photogrammetry. *The Cryosphere*, 9: 229-243, doi:10.5194/tc-9-229-2015.

Carboneau, P.E., Dietrich, J.T., 2016. Cost-effective non-metric photogrammetry from consumer-grade sUAS: implications for direct georeferencing of structure from motion photogrammetry. *Earth Surf. Process. Landforms*, 42(3): 473-486.

Clapuyt, F., Vanacker, V., Van Oost, K., 2016. Reproducibility of UAV-based earth topography reconstructions based on Structure-from-Motion algorithms. *Geomorphology*, 260: 4-15.

Colomina, I., Molina, P., 2014. Unmanned aerial systems for photogrammetry and remote sensing: A review. *ISPRS Journal of Photogrammetry and Remote Sensing*, 92: 79-97.

D'Agata, C., Bocchiola, D., Maragno, D., Smiraglia, C., Diolaiuti, G.A., 2014. Glacier shrinkage driven by climate change during half a century (1954–2007) in the Ortles-Cevedale group (Stelvio National Park, Lombardy, Italian Alps). *Theor Appl Climatol*, 116, 169-190.

Dall'Asta, E., Delaloye, R., Diotri, F., Forlani, G., Fornari, M., Morra di Cella, U., Pogliotti, P., Roncella, R., Santise, M., 2016. Unmanned Aerial Systems and DSM matching for rock glacier monitoring. *ISPRS Journal of Photogrammetry and Remote Sensing*, available online at www.sciencedirect.com/science/journal/aip/09242716.

Diolaiuti, G.A., Smiraglia, C., 2010. Changing glaciers in a changing climate: how vanishing geomorphosites have been driving deep changes in mountain landscapes and environments. *Géomorphologie: relief, processus, environnement*, 2: 131-152.

Eltner, A., Kaiser, A., Castillo, C., Rock, G., Neugirg, F., Abellán, A., 2015. Image-based surface reconstruction in geomorphometry – merits, limits and developments. *Earth Surface Dynamics*, 4: 359-389.

Forlani, G., Pinto, L., Roncella, R., Pagliari, D., 2014. Terrestrial photogrammetry without ground control points. *Earth Science Informatics*, 7: 71-81.

Forlani, G., Roncella, R., Diotri, F., 2015. Production of high-resolution digital terrain models in mountain regions to support risk assessment. *Geomatics, Natural Hazards and Risk*, 6(5-7): 379-397.

Fugazza, D., Senese, A., Azzoni, R.S., Smiraglia, C., Cernuschi, C., Severi, D., Diolaiuti, G.A., 2015. High-resolution mapping of glacier surface features. The UAV survey of the Forni Glacier (Stelvio National Park, Italy). *Geografia Fisica e Dinamica del Quaternario*, 38: 25-33.

Fugazza, D., Senese, A., Azzoni, R.S., Maugeri, M., Diolaiuti, G.A., 2016. Spatial distribution of surface albedo at the Forni Glacier (Stelvio National Park, Central Italian Alps). *Cold Regions Science and Technology*, 125: 128-137.

Fugazza, D., Scaioni, M., Corti, M., D'Agata, C., Azzoni, R.S., Cernuschi, C., Smiraglia, C., Diolaiuti, G., 2017. Combination of UAV and terrestrial photogrammetry to assess rapid glacier evolution and conditions of glacier hazards. *Natural Hazards Earth System Science Discussion*, available at <https://doi.org/10.5194/nhess-2017-198> (last access on 10th Jul 2017), in review.

- Gómez-Gutiérrez, Á., de Sanjosé-Blasco, J. J., de Matías-Bejarano, J., Berenguer-Sempere, F., 2014. Comparing two photoreconstruction methods to produce high density point clouds and DEMs in the Corral del Veleta Rock Glacier (Sierra Nevada, Spain). *Remote Sensing*, 6: 5407-5427.
- Gómez-Gutiérrez, Á., de Sanjosé-Blasco, J. J., Lozano-Parra, J., Berenguer-Sempere, F., de Matías-Bejarano, J., 2015. Does HDR pre-processing improve the accuracy of 3-D models obtained by means of two conventional SfM-MVS software packages? The case of the Corral del Veleta Rock Glacier. *Remote Sensing*, 7: 10269-10294.
- Gu, Z., Feng, T., Scaioni, M., Wu, H., Liu, J., Tong, X., Li, R., 2014. Experimental Results of Elevation Change Analysis in the Antarctic Ice Sheet Using DEMs from ERS and ICESat Data. *Annals of Glaciology*, 55(66): 198-204, doi: 10.3189/2014AoG66A124.
- Heid, T., Kääh, A., 2012. Evaluation of Existing Image Matching Methods for Deriving Glacier Surface Displacements Globally from Optical Satellite Imagery. *Remote Sensing of Environment*, 118: 339-355.
- Immerzeel, W.W., Kraaijenbrink, P.D.A., Shea, J.M., Shrestha, A.B., Pellicciotti, F., Bierkens, M.F.P., de Jong, S.M., 2014. High-resolution monitoring of Himalayan glacier dynamics using unmanned aerial vehicles. *Remote Sensing of Environment*, 150:93-103.
- Jaboyedoff, M., Oppikofer, T., Abellán, A., Derron, M.H., Loye, A., Metzger, R., Pedrazzini, A., 2012. Use of LIDAR in landslide investigations: A review. *Natural Hazards*, 61: 1-24.
- James, M.R., Robson, S., Smith, M.W., 2017. 3-D uncertainty-based topographic change detection with structure-from-motion photogrammetry: precision maps from ground control and directly georeferenced surveys. *Earth Surface Processing and Landforms*, available online at <https://doi.org/10.1002/esp.4125> (last access on 10th Jul 2017).
- Kääh, A., Girod, L., Berthling, I., 2014. Surface kinematics of periglacial sorted circles using structure-from-motion technology. *Cryosphere*, 8: 1041-1056.
- Kraaijenbrink, P.D.A., Shea, J.M., Pellicciotti, F., de Jong, S.M., Immerzeel, W.W., 2016. Object-based analysis of unmanned aerial vehicle imagery to map and characterize surface features on a debris-covered glacier. *Remote Sensing of Environment*, 186: 581-595.
- Lane, S., Richard, K.S., Chandler, J.H., 1993. Developments in Photogrammetry – The Geomorphological Potential. *Progress in Physical Geography*, 17(3): 306-328.
- Li, R., Ye, W., Qiao, G., Tong, X., Liu, S., Kong, F., Ma, X., 2017. A New Analytical Method for Estimating Antarctic Ice Flow in the 1960s From Historical Optical Satellite Imagery. *IEEE Trans. Geoscience Remote Sensing*, 55(5): 2771-2785.
- Mosbrucker, A.R., Major, J.J., Spicer, K.R., Pitlick, J., 2017. Camera system considerations for geomorphic applications of SfM photogrammetry. *Earth Surf. Process. Landforms*, 42: 969–986. doi:10.1002/esp.4066.
- O'Connor, J., Smith, M.J., James, M.R., 2017. Cameras and settings for aerial surveys in the geosciences: optimising image data. *Progress in Physical Geography*, available online at <https://doi.org/10.1177/0309133317703092>.
- Piermattei, L., Carturan, L., Guarnieri, A., 2015. Use of terrestrial photogrammetry based on structure from motion for mass balance estimation of a small glacier in the Italian Alps. *Earth Surf. Proc. Land.*, 40: 1791-1802, doi: 10.1002/esp.3756, 2015.
- Piermattei, L., Carturan, L., de Blasi, F., Tarolli, P., Dalla Fontana, G., Vettore, A., Pfeifer, N., 2016. Suitability of ground-based SfM–MVS for monitoring glacial and periglacial processes. *Earth Surface Dynamics*, 4: 325-443, doi: 10.5194/esurf-4-425-2016.
- Ryan, J.C., Hubbard, A.L., Box, J.E., Todd, J., Christoffersen, P., Carr, J.R., Holt, T.O., Snooke, N., 2015. UAV photogrammetry and structure from motion to assess calving dynamics at Store Glacier, a large outlet draining the Greenland ice sheet. *Cryosphere*, 9: 1-11, doi:10.5194/tc-9-1-2015.
- Scaioni, M., Longoni, L., Melillo, V., Papini, M., 2014. Remote Sensing for Landslide Investigations: An Overview of Recent Achievements and Perspectives. *Remote Sensing*, 6(10): 9600-9652, doi: 10.3390/rs6109600.
- Smiraglia, C., Azzoni, R.S., D'Agata, C., Maragno, D., Fugazza, D., Diolaiuti, G.A., 2015. The evolution of the Italian glaciers from the previous data base to the new Italian inventory. preliminary considerations and results. *Geografia Fisica e Dinamica del Quaternario*, 38: 79-87 doi: 10.4461/GFDQ.2015.38.08, 2015.
- Tonkin, T.N., Midgley, N.G., Graham, D.J., Labadz, J.C., 2014. The potential of small unmanned aircraft systems and structure-from-motion topographic surveys: A test of emerging integrated approaches at Cwm Idwal, North Wales. *Geomorphology*, 226: 35-43.
- Westoby, M.J., Brasington, J., Glasser, N.F., Hambrey, M.J., Reynolds, J.M., 2012. "Structure-from-Motion" Photogrammetry: A low-cost, effective tool for geoscience applications. *Geomorphology*, 179: 300-314.
- Whitehead, K., Moorman, B.J., Hugenholtz, C.H. Brief Communication: Low-cost, on-demand aerial photogrammetry for glaciological measurement. *The Cryosphere*, 7: 1879-1884.

References from books:

Heritage, G.L., Large, A.R.G., 2009. *Laser Scanning for the Environmental Sciences*. John Wiley & Sons, Chichester, U.K., 302 pp.

Luhmann, T., Robson, S., Kyle, S., Boehm, J., 2014. *Close Range Photogrammetry: 3D Imaging Techniques – 2nd Edition*. Walter De Gruyter Inc., Germany, 684 pages.

References from Other Literature:

Barazzetti L., Forlani G., Remondino, F., Roncella, R., Scaioni, M., 2011. Experiences and achievements in automated image sequence orientation for close-range photogrammetric projects. In: Proc. Int. Conf. 'Videometrics, Range Imaging, and Applications XI', 23-26 May, Munich (Germany), Proc. of SPIE, Vol. 8085, paper No. 80850F, 13 pp. (e-doc), DOI: 10.1117/12.890116, 2011.

Rutzinger, M., Höfle, B., Lindenbergh, R., Oude Elberink, S., Pirotti, F., Sailer, R., Scaioni, M., Stötter, J., Wujanz, D., 2016. Close-Range Sensing Techniques in Alpine Terrain. *ISPRS Ann. Photogramm. Remote Sens. Spatial Inf. Sci.*, Vol. III, Part 6, pp. 15-22, DOI: 10.5194/isprs-annals-III-6-15-2016.

Scaioni, M., Tong, X., Li, R., 2013. Application of GLAS laser altimetry to detect elevation changes in East Antarctica. *ISPRS Ann. Photogramm. Remote Sens. Spatial Inf. Sci.*, Vol. II, Part 5/W2, pp. 253-258, doi: 10.5194/isprsannals-II-5-W2-253-2013.

Solbø, S., Storvold, R., 2013. Mapping Svalbard Glaciers with the cryowing UAS. *Int. Arch. Photogramm. Remote Sens. Spatial Inf. Sci.*, Vol. XL, Part. 1/W2, pp. 373-377.

Wenzel, K., Rothmel, M., Fritsch, D., Haala, N., 2013. Image acquisition and model selection for multi-view stereo. *Int. Arch. Photogramm. Remote Sens. Spatial Inf. Sci.*, Vol. XL, Part 5W, pp. 251-258.